Phys. Status Solidi C **11**, No. 3–4, 714–717 (2014) / **DOI** 10.1002/pssc.201300434

physica status solidi c
www.pss-c.com
current topics in solid state physics

Temperature-dependent *ac* current-voltage-capacitance characteristics of GaN-based light-emitting diodes under high forward bias

Wei Yang[1], Ding Li[1], Juan He[1], Cunda Wang[1,2], and Xiaodong Hu[*,1]

[1] State Key Laboratory for Artificial Microstructure and Mesoscopic Physics, School of Physics, Peking University, Beijing 100871, P.R. China
[2] Department of Applied Physics, Tianjin University, Tianjin 300072, P.R. China

Received 21 August 2013, revised 17 January 2014, accepted 20 January 2014
Published online 21 March 2014

Keywords light-emitting diodes, admittance, junction voltage, Poole-Frenkel effect

* Corresponding author: e-mail huxd@pku.edu.cn, Phone: +86-10-62767621

Temperature-dependent *ac* current-voltage-capacitance characteristics between 90 K and 440 K were investigated for InGaN/GaN multi-quantum-wells blue light-emitting diodes (LEDs) under high forward bias. Under large forward current, deep saturation of junction voltage V_j was observed over a wide temperature range. It was found that V_j corresponds to the separation energy of electron and hole quasi-Fermi levels and its temperature dependence could be well explained by the flat band model. After the pinning of quasi-Fermi levels, the forward current is dominated by the drift current in the *p*-GaN access layer. Considering Poole-Frenkel effect, a quantitative model was developed to reproduce the current-voltage characteristics of LEDs under high forward bias.

1 Introduction GaN-based light-emitting diodes (LEDs) are expected to become the general illumination sources used in solid-state lighting in replacement of incandescent and fluorescent lamps [1]. Measurement and analysis of current-voltage-capacitance (IVC) characteristics will establish direct links between material parameters and device performances. Using the conventional model, some fundamental parameters of diodes can be obtained, such as turn-on voltage, reverse leakage current and ideality factor [2]. Inspection of the I-V curve allows for quick diagnosis of potential problems within devices [3]. However, previous researchers mainly studied the current-voltage dependence under low or intermediate forward bias. For example, Fedison *et al*. attributed the abnormal electrical behavior at low forward bias to the presence of deep-level traps at the junction [4]. Reynolds *et al*. compared I-V curves in intermediate bias regimes to obtain an understanding of the tunneling entities involved [5]. Besides, capacitance-voltage (C-V) characteristics were often measured, but under reverse biases to study the carrier concentration profile in hetero-structure or quantum wells [6, 7], and there was little study on the capacitance of LED devices under forward bias [8]. However, most applications of LED devices require them to be driven under high forward bias with large injection current. Therefore, it is of significance to study the IVC characteristics under high forward bias and also its temperature-dependent behavior.

In this paper, temperature-dependent current-voltage-capacitance characteristics under high forward bias were investigated for InGaN/GaN multi-quantum-wells (MQWs) blue LEDs between 90 K and 440 K. Based on the *ac*-IV method proposed recently [9], junction voltage V_j was retrieved from temperature-dependent *ac* admittance small signal measurement. Under large forward current, deep saturation of V_j was observed over a wide temperature range. A theoretical model considering Poole-Frenkel effect was also proposed to reproduce the I-V curve quantitatively. This model enabled us to gain enhanced insight into the current-voltage characteristic of GaN-based LEDs and also other devices such as laser diodes.

2 Experiments Conventional GaN-based LEDs with peak emission wavelength of 456 nm were grown on sapphire substrate using metal-organic chemical vapor deposi-

tion. Trimethylgallium, trimethylindium, and ammonia were used as the precursors for Ga, In, and N sources, respectively. The epi-structure consists of a 0.5 µm thick undoped GaN layer, a 3.5 µm thick Si doped *n*-type GaN layer, a five period un-doped $In_{0.18}Ga_{0.82}N$/GaN MQWs (2.5 nm/7 nm) active region and a 200 nm thick *p*-type Mg doped GaN layer. The LED chips were fabricated with a standard LED process by photolithography and inductively coupled plasma reactive ion etching (RIE). Contacts consisting of a Cr/Pt/Au multilayer and indium tin oxide (ITO), which performs a current spreading function, were deposited onto the *n*-GaN and *p*-GaN layers, respectively. The chips were encapsulated with silicone for subsequent measurements.

For measurement of the electrical behaviors, the LED chip was mounted on an alumina ceramic substrate with Ag charged epoxy. The sample was then stuck on the head of a liquid nitrogen cryostat (90-440 Kelvin). The temperature-dependent I-V and admittance measurements were carried out by an Agilent 4155C semiconductor parameter analyzer and an Agilent 4294A precision impedance analyzer respectively. The Hall-effect measurement was also performed using van der Pauw geometry to investigate hole concentration and mobility.

3 Results and discussion Figure 1 shows the forward I-V curve of a typical LED at room temperature (RT) plotted in semi-logarithmic scale. Under low forward bias (V<1.5 V), the current is dominated by leakage current, which occurs primarily at open-core screw dislocations [10], local deep-level states in *p*-GaN generated during the passivation [11] and/or mesa sidewalls induced during RIE process [12]. In intermediate bias range (1.5 V<V<3 V), two successive linear parts of I-V curve was observed, and this feature showed little temperature-dependence (the temperature-dependent I-V curves in this bias range are not shown). The effective ideality factor in intermediate bias range has been reported in the range of 3-12, which led to the conclusion that tunneling is the dominant mechanism at this bias level [13]. Tunneling energies on the order of 200 and 100 meV have been attributed to heavy hole tunneling and defect/dislocation induced deep level states assisted electron tunneling, respectively [5, 14]. The defect distribution and its charge dependence within the layer structure and/or the large valence band off-set may explain the change of different tunneling entities [15–17]. Because the forward tunneling current has been extensively studied in Ref. [5, 14–17], in this paper we will focus our study only under high bias regime as shown in the shaded area of the I-V curve in Fig. 1 (the inset shows the temperature-dependence of the shaded area).

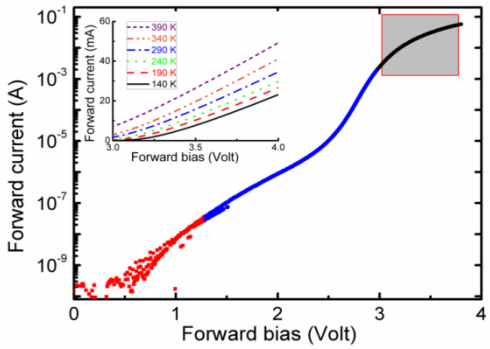

Figure 1 Typical room temperature I-V curve of a GaN-based blue LED. The inset shows enlarged I-V curves under high bias regime (the shaded area) at different temperatures.

The forward *ac* admittance characteristics were measured under a small modulation signal with an oscillation level of 50 mV and the detailed measuring model can be found in our previous publications [9, 18]. The frequency of the small signal and the measuring temperature were varied during the experiments. The inset of Fig. 2 shows the apparent capacitance at 340 K for various modulation frequencies. The apparent capacitance shows a "negative" value under large forward bias, which is always accompanied by light emission and can be interpreted in terms of carrier recombination and "reclaimable" charge [18, 19]. The negative capacitance (NC) is more noticeable at lower modulation frequencies, because at higher frequencies, more carriers are "frozen" due to finite inertia [20]. Unless otherwise stated, the modulation frequency of small signal is fixed at 100 kHz for following measurements. Figure 2 shows the apparent capacitance (left) and conductance (right) at different temperatures versus forward bias. The absolute value of NC increases as the temperature increases. The possible reason is that more shallow acceptors become ionized as temperature increases and the ionized free holes contribute to the high frequency capacitance [7].

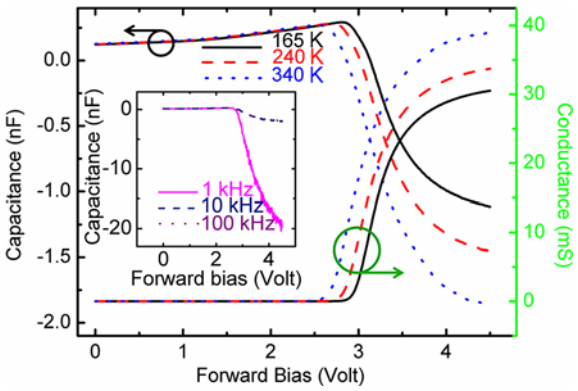

Figure 2 Apparent capacitance (left) and conductance (right) versus forward bias at different temperature (the modulation frequency is fixed at 100 kHz) and inset shows capacitance at 340 K for various modulation frequencies.

The ac-IV method was employed to characterize the electrical behavior of a semiconductor diode in detail [9]. The junction voltage V_j can be extracted via the results of *ac* admittance measurement (shown in Fig. 2) combined with direct current (dc) I-V plotting (shown in Fig. 1). This procedure was done for the temperature range from 165 K to 440 K. We found that the junction voltage deeply saturates at all measured temperatures (as shown in Fig. 3). The saturation value of V_j decreases as temperature increases. Based on the flat band model of *p-n* junction (the case of MQWs is similar) [21], the junction voltage corresponds to the separation energy of quasi-Fermi levels of electrons and holes around the active region:

$$qV_j = E_g - k_B T \ln \frac{np}{N_C N_V} \quad , \tag{1}$$

where q is the elementary charge, E_g is the band-gap of semiconductor, k_B the Boltzmann constant, n (p) is the electron (hole) concentration and N_C (N_V) the effective density of states in the conduction (valence) band. Note that the band-gap E_g also shrinks with increasing temperature and it follows the Varshni formula [14]. Therefore, Eq. (1) can be written as

$$E_g(T) - qV_j = k_B T \ln \frac{np}{N_C N_V} \quad . \tag{2}$$

If the slowly varying temperature dependence on the right term of Eq. (2) is neglected, a linear relationship of the left term with temperature can be obtained (as shown in the inset of Fig. 3).

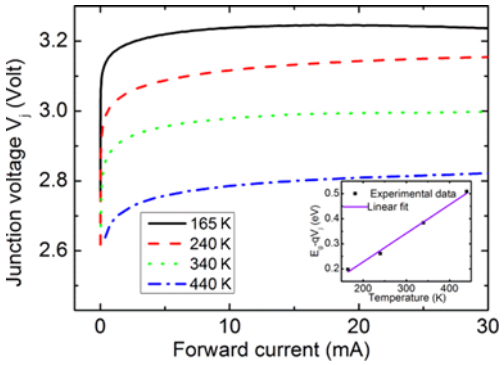

Figure 3 Junction voltage versus forward current at different temperatures and the inset is a linear fit of (E_g-qV_j) versus temperature.

Under high forward injection current, the deep saturation of junction voltage V_j implies the pinning of quasi-Fermi levels across the active region [22]. The current is thus mainly limited by the series resistor involving the neutral *n*-GaN and *p*-GaN access zones of the diode on both sides of the space charge zones. For Mg doped GaN, the hole concentration is given by [23]

$$p = \frac{N_A}{1 + \frac{pg}{N_V}\exp(\frac{\Delta E_A}{k_B T})} - N_{comp} \, , \tag{3}$$

where N_A and ΔE_A are concentration and activation energy of acceptor, respectively, g=2 is degeneracy factor, and N_{comp} is the concentration of compensating donors. The electron concentration in *n*-GaN can be estimated using similar expression as Eq. (3). Since holes have a significantly lower mobility than electrons, the resistivity of *p*-GaN is much higher than that of *n*-GaN. Therefore the potential drop takes place mostly in the *p*-GaN layer, as shown in the band diagram of the LED junction in Fig. 4. The resulting electric field F_p given by F_p=(V-V_j)/t_p (t_p is the thickness of access p-GaN layer) is on the order of 10^4 V/cm. In that case of high electric fields, an increase of electrical conductivity (decrease of ionization energy of carriers) is represented by the Poole-Frenkel effect [12, 24]. Considering the lowering of activation energy by the Poole-Frenkel effect, the resulting potential barrier is

$$\Delta E_A = \Delta E_A^0 - \beta_{PF} F_p^{1/2} \quad . \tag{4}$$

In Eq. (4), β_{PF} is the Poole-Frenkel coefficient: $\beta_{PF} = (q^3/4\pi\varepsilon_\infty)^{1/2}$, where ε_∞ is the high frequency permittivity.

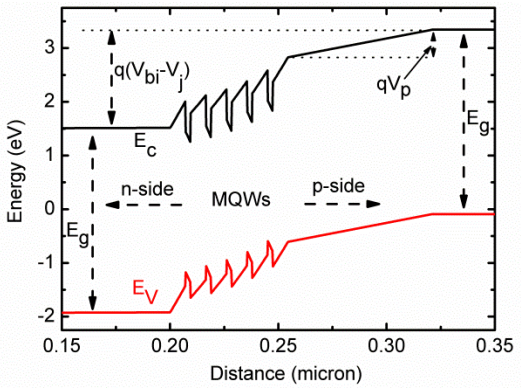

Figure 4 Schematic diagram of the band structure of LED junction under forward bias.

The Poole-Frenkel effect was observed under high injection regime [12], therefore should be taken into consideration for further analysis of I-V curve. Drift current depends on the concentration p and mobility μ_p of charged carriers (holes) and also the electric field F_p in the *p*-GaN layer. Accordingly, the current density, J=$qp\mu_p F_p$, with hole concentration p deduced from Eq. (3), the drift current is given by

$$I = SN_V \frac{N_A - N_{comp}}{N_{comp}} q\mu_p F_p \exp\left(-\frac{\Delta E_A^0}{k_B T}\right) \exp\left(\frac{\beta_{PF} F_p^{\frac{1}{2}}}{k_B T}\right), \tag{5}$$

where S is the size of the LED chip (S=272×249 μm^2 is measured using an optical microscope), and the current density is assumed to be uniform across this area. Figure 5 shows the result of nonlinear least square fitting of *I-V* curve at RT using Eq. (5), in which $\varepsilon_\infty = 5.4$ and $\Delta E_A^0 = 210$ meV is adopted from Ref. [25], and

$N_{comp}/N_A = 1/10$ is adopted from Ref. [26]. From the simulation procedure, the saturation of junction voltage is determined to be 3.01 V, which agrees well with that V_j=2.99 V shown in the inset of Fig. 5 extracted by ac-IV method. Reproducing the I-V curves in high conduction regime gives hole mobility μ_p=2.96 cm^2/(V·s), and this value is consistent with that of Hall-effect measurement.

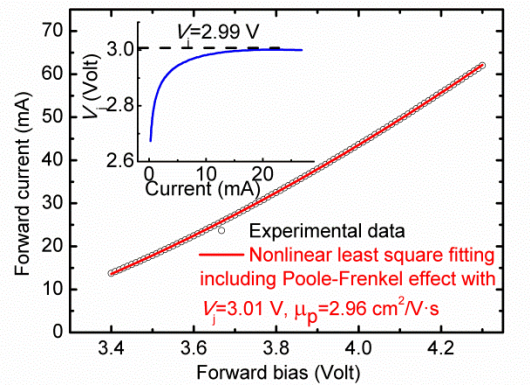

Figure 5 Experimental I-V curve at large forward current, and red solid line is fitted theoretical curve. The inset shows dependence of junction voltage on forward current.

4 Conclusions The temperature-dependent *ac* current-voltage-capacitance characteristics of GaN-based blue LEDs are quantitatively studied under high bias regime. Based on the *ac*-IV method, deep saturation of junction voltage V_j was observed over a wide temperature range. V_j corresponds to the separation energy of quasi-Fermi levels of electrons and holes and its temperature dependence could be well explained by the flat band model of conventional *p*-*n* junction theory. After the pinning of quasi-Fermi levels, the forward current is dominated by the drift current in the *p*-GaN access layer. Considering Poole-Frenkel effect, a quantitative model was developed to reproduce the current-voltage characteristics of LEDs under high forward bias.

Acknowledgements This work is supported by the National Natural Science Foundation of China under Grant Nos. 51102003 and 60990313. The author is grateful to Dr. Johannes Herrnsdorf and Dr. Enyuan Xie in University of Strathclyde for helpful discussions.

References

[1] S. Pimputkar, J. S. Speck, S. P. DenBaars, and S. Nakamura, Nature Photon. **3**, 180 (2009).
[2] E. Schubert, Light Emitting Diodes, 2nd ed. (Cambridge University Press, 2006).
[3] J. M. Shah, Y.-L. Li, Th. Gessmann, and E. F. Schubert, J. Appl. Phys. **94**, 2627 (2003).
[4] J. B. Fedison, T. P. Chow, H. Lu, and I. B. Bhat, Appl. Phys. Lett. **72**, 2481 (1998).
[5] Jr. C. L. Reynolds and A. Patel, J. Appl. Phys. **103**, 086102 (2008).
[6] T.S. Kim, B.J. Ahn, Y. Dong, K.N. Park, J.-G. Lee, Y. Moon, H.-K. Yuh, S.-C. Choi, J.-H. Lee, S.-K. Hong, and J.-H. Song, Appl. Phys. Lett. **100**, 071910 (2012); O. A. Soltanovich, N. M. Shmidt, and E. B. Yakimov, Semiconductors **45**, 221 (2011).
[7] Y. Zohta, H. Kuroda, R. Nii, and S. Nakamura, J. Cryst. Growth **189–190**, 816 (1998).
[8] O. Soltanovich and E. Yakimov, Phys. Status Solidi C **10**, 338 (2013); K. Bansal and S. Datta, Appl. Phys. Lett. **102**, 053508 (2013); M. Anutgan, and I. Atilgan, Appl. Phys. Lett. **102**, 153504 (2013).
[9] C.Y. Zhu, C.D. Wang, L.F. Feng, G.Y. Zhang, L.S. Yu, and J. Shen, Solid-State Electron. **50**,821 (2006).
[10] S. W. Lee, D. C. Oh, H. Goto, J. S. Ha, H. J. Lee, T. Hanada, M. W. Cho, T. Yao, S. K. Hong, H. Y. Lee, S. R. Cho, J. W. Choi, J. H. Choi, J. H. Jang, J. E. Shin, and J. S. Lee, Appl. Phys. Lett. **89**, 132117 (2006).
[11] H. Kim, J. Cho, Y. Park, and T.-Y. Seong, Appl. Phys. Lett. **92**, 092115 (2008).
[12] L. Hirsch and A. S. Barriere, J. Appl. Phys. **94**, 5014 (2003).
[13] H. C. Casey, Jr., J. Muth, S. Krishnankutty, and J. M. Zavada, Appl. Phys. Lett. **68** 2867 (1996); A. Chitnis, A. Kumar, M. Shatalov, V. Adivarahan, A. Lunev, J. W. Yang, G. Simin, M. Asif Khan, R. Gaska, and M. Shur, Appl. Phys. Lett. **77**, 3800 (2000); X. A. Cao, E. B. Stokes, P. M. Sandvik, S. F. LeBoeuf, J. Kretchmer, and D. Walker, IEEE Electron Device Lett. **23**, 535 (2002).
[14] D. Yan, H. Lu, D. Chen, R. Zhang, and Y. Zheng, Appl. Phys. Lett. **96**, 083504 (2010).
[15] S.-H. Han, D.-Y. Lee, H.-W. Shim, J. W. Lee, D.-J. Kim, S. Yoon, Y. S. Kim, and S.-T. Kim, Appl. Phys. Lett. **102**, 251123 (2013).
[16] J. Kim, Y. Tak, J. Kim, S. Chae, J.-Y. Kim, and Y. Park, J. Appl. Phys. **114**, 013101 (2013).
[17] K. B. Lee, P. J. Parbrooky, T. Wang, J. Bai, F. Ranalli, R. J. Airey, and G. Hill, Phys. Status Solidi B **247**, 1761 (2010).
[18] L. F. Feng, Y. Li, C. Y. Zhu, H. X. Cong, and C. D. Wang, IEEE J. Quantum Electron. **46**, 1072 (2010).
[19] S. E. Laux and K. Hess, IEEE Trans. Electron Devices **46**, 396 (1999).
[20] M. Ershov, H. C. Liu, L. Li, M. Buchanan, Z. R. Wasilewski, and A. K. Jonscher, IEEE Trans. Electron Devices **45**, 2196 (1998).
[21] S. M. Sze and K. K. Ng, Physics of Semiconductor Devices, 3rd ed. (Wiley, New York, 2006).
[22] L. F. Feng, D. Li, C. Y. Zhu, and C. D. Wang，H. X. Cong, G. Y. Zhang, and W. M. Du, J. Appl. Phys. **102**, 094511 (2007).
[23] W. Götz, R. S. Kern, C. H. Chen, H. Liu, D. A. Steigerwald, and R. M. Fletcher, Mater. Sci. Eng. B **59**, 211 (1999).
[24] J. G. Simmons, Phys. Rev. **155**, 657 (1967).
[25] http://www.ioffe.ru/SVA/NSM/Semicond/.
[26] U. Kaufmann, P. Schlotter, H. Obloh, K. Köhler, and M. Maier, Phys. Rev. B **62**, 10867 (1998).